The linear velocity field of SDSS DR7 galaxies: constraints on flow amplitudes and the growth rate

Martin Feix[*]

Department of Physics, Israel Institute of Technology - Technion, Haifa 32000, Israel
E-mail: mfeix@physics.technion.ac.il

Large-scale peculiar motion modulates the observed luminosity distribution of galaxies. Using about half a million SDSS galaxies, this can be harnessed to obtain bounds on peculiar velocity moments, the amplitude of the linear matter power spectrum, σ_8, and the growth rate of density perturbations at $z \sim 0.1$. Results obtained from this approach agree well with the predictions of the ΛCDM model and are consistent with the reported $\sim 1\%$ zero-point tilt in the SDSS photometry.

---

[*]Speaker.

1. Introduction

If the standard paradigm of cosmology is correct, the observed structure of the universe originated from tiny density fluctuations via gravitational instability. The clustering process is inevitably associated with peculiar motions of matter, i.e. deviations from a pure Hubble flow, which exhibit a coherent pattern on large scales. Since galaxies can, to good approximation, be treated as test particles, they should appropriately reflect the underlying peculiar velocity field which contains valuable information for constraining and discriminating between different cosmological models.

Redshifts of galaxies are systematically altered by the line-of-sight components of their peculiar velocities and differ from their actual distances. Consequently, intrinsic galaxy luminosities inferred from the observed flux using redshifts rather than distances appear brighter or dimmer. Since this effect is obscured by the natural scatter in the distribution of magnitudes, it cannot be used to derive the peculiar velocities of individual galaxies. However, it is possible to approach peculiar velocities in a statistical sense by constraining the parameters of some appropriate, predefined velocity model. For instance, constraints on the bulk motion of galaxies in a subvolume of a given survey can be derived by comparing the luminosity distribution of galaxies in the subvolume with that of the whole survey. Reconstructing the linear velocity field from the observed density field in redshift space, this technique further provides a way of estimating the growth rate of density perturbations which is independent from the apparent clustering anisotropy of galaxies [1, 2].

Below I briefly review the luminosity-based approach outlined above and discuss its recent application to galaxy data from the Sloan Digital Sky Survey (SDSS) [3]. Methods of this kind have first been adopted to estimate the motion of Virgo relative to the Local Group [4], and more recently, to constrain bulk flows and the growth rate in the local universe within $z \sim 0.01$ [5, 6].

2. Velocity-induced modulation of observed galaxy luminosities

Due to inhomogeneities, the observed redshift z of a galaxy is generally different from its cosmological one, z_c, which is defined for the homogeneous background. In linear perturbation theory, the two quantities are connected through [7]

$$\frac{z - z_c}{1 + z} = \frac{V(t,r)}{c} - \frac{\Phi(t,r)}{c^2} - \frac{2}{c^2} \int_{t(r)}^{t_0} dt \frac{\partial \Phi[\hat{r}r(t), t]}{\partial t} \approx \frac{V(t,r)}{c},$$

where $\hat{r}$ denotes a unit vector along the line of sight to the galaxy, V is the galaxy's (physical) radial peculiar velocity, and Φ the usual gravitational potential. Focusing on low redshifts at the present time, the velocity V is explicitly assumed as the dominant contribution. All fields are considered relative to their present-day values at t_0. The difference in redshifts enters the distance modulus $\mathrm{DM} = 25 + 5\log_{10}[D_L/\mathrm{Mpc}]$ and causes the observed absolute magnitudes M to deviate from their true values $M^{(t)}$, i.e.

$$M = m - \mathrm{DM}(z) - K(z) + Q(z) = M^{(t)} + 5\log_{10}\frac{D_L(z_c)}{D_L(z)},$$

where m is the apparent magnitude, D_L is the luminosity distance, and the functions $Q(z)$ and $K(z)$ account for luminosity evolution and K-correction [8], respectively. Restricted to scales where

linear theory is valid, $M - M^{(t)}$ varies systematically over the sky, and thus provides a probe of the cosmic velocity field.

Given a galaxy survey with magnitudes, (spectroscopic) redshifts, and angular positions $\hat{r}_i$ on the sky, the idea is to choose an appropriate parameterized model of $V(\hat{r}, z)$ and to maximize the probability of the data,

$$P_{\text{tot}} = \prod_i P(M_i | z_i, V(\hat{r}_i, z_i)) = \prod_i \left(\phi(M_i) \middle/ \int_{M_i^+}^{M_i^-} \phi(M) \mathrm{d}M \right),$$

where redshift errors are neglected [5]. Here $\phi(M)$ denotes the galaxy luminosity function (LF), and the limiting magnitudes $M^{\pm}$ depend on the cosmological redshift z_c, and hence on $V(\hat{r}, z)$. The motivation of this approach is to find those velocity model parameters which minimize the spread in the observed magnitudes.

3. Constraints from SDSS galaxy luminosities at z ~ 0.1

Galaxy data from the SDSS Data Release 7 [9] trace the cosmic velocity field out to $z \sim 0.1$. Here I summarize recent results obtained from applying the luminosity method to suitable subsets comprising up to half a million galaxies [10, 11].

Data.—The analysis is based on the latest version of the NYU Value-Added Galaxy Catalog (NYU-VAGC), adopting the subsample `safe` to minimize incompleteness and systematics [12]. Using Petrosian $^{0.1}r$-band magnitudes, only galaxies with $14.5 < m_r < 17.6$, $-22.5 < M_r - 5\log_{10} h < -17.0$, and $0.02 < z < 0.22$ (relative to the CMB frame) are included. In addition, galaxy mock catalogs were built to study errors and known systematics of the data.

Radial velocity model.—Constraints on velocity moments and derived quantities assume a bin-averaged model $\tilde{V}(\hat{r})$ in two redshift bins, $0.02 < z < 0.07$ and $0.07 < z < 0.22$. For each bin, the velocity field was decomposed into spherical harmonics, i.e.

$$a_{lm} = \int \mathrm{d}\Omega \tilde{V}(\hat{r}) Y_{lm}(\hat{r}), \qquad \tilde{V}(\hat{r}) = \sum_{l,m} a_{lm} Y_{lm}^*(\hat{r}), \qquad l > 0,$$

where the sum over l is cut at some maximum value $l_{\max}$. Because the SDSS data cover only part of the sky, the inferred a_{lm} are not statistically independent. The impact of the angular mask was studied with the help of suitable galaxy mock catalogs. The monopole term ($l = 0$) was not included since it is degenerate with an overall shift of magnitudes.

LF estimators.—Reliable measurements of the galaxy LF form a key step in the analysis. To assess the robustness of results with respect to different LF models, the data were examined using LF estimators based on a Schechter form and a more flexible spline-based model, together with several combinations and variations thereof. For simplicity, a linear dependence of the luminosity evolution with redshift was assumed.

Bulk flows and higher-order velocity moments.—Accounting for known systematic errors in the SDSS photometry, measurements of "bulk flows" are consistent with a standard ΛCDM cosmology at a 1–2σ confidence level in both redshift bins. A joint analysis of the corresponding three Cartesian components confirms this result. To characterize higher-order moments, direct
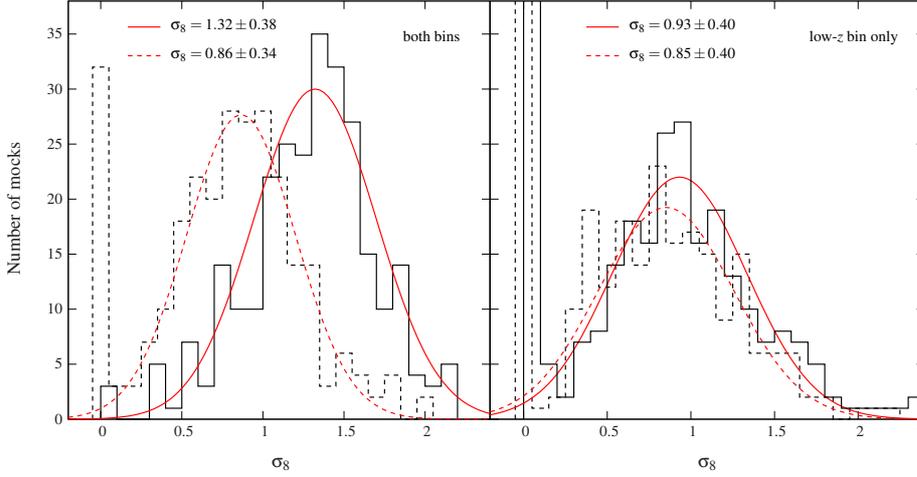
Figure 1: Estimates of σ_8 from galaxy mocks: shown are the recovered distributions and respective Gaussian fits with (solid lines) and without (dashed lines) the inclusion of a (randomly oriented) photometric tilt, using the information in both redshift bins (left) and the low-z bin only (right).

constraints on the angular velocity power spectrum $C_l = \langle |a_{lm}|^2 \rangle$ were obtained up to the octupole contribution. The estimated C_l were found compatible with the theoretical power spectra of the ΛCDM cosmology.

Constraints on σ_8.—Assuming a prior on the C_l as dictated by the ΛCDM model with fixed Hubble constant and density parameters, the amplitude of the velocity field was estimated in terms of σ_8. Because of a dipole-like tilt in the galaxy magnitudes [13], raw estimates of σ_8 were biased toward larger values (see Figure 1). After correcting for this magnitude tilt, it was found that $\sigma_8 = 1.1 \pm 0.4$ for the combination of both redshift bins and $\sigma_8 = 1.0 \pm 0.5$ for the low-z bin only, where the low accuracy is due to the limited number of galaxies.

The linear growth rate.—Modeling the linear velocity field from the observed galaxy clustering in redshift space, the luminosity approach is capable of constraining the growth rate of density perturbations, $\beta = f(\Omega)/b$, where b is the linear galaxy bias [6]. To this end, both magnitude- and volume-limited subsamples were selected over a rectangular patch (in survey coordinates) within the range $0.06 < z < 0.12$. Following [14], the velocity reconstruction was done in "harmonic" space by smoothing the density field with a Gaussian kernel of $10h^{-1}$ Mpc radius and solving

$$\frac{1}{s^2}\frac{\mathrm{d}}{\mathrm{d}s}\left(s^2\frac{\mathrm{d}\Phi_{lm}}{\mathrm{d}s}\right) - \frac{1}{1+\beta}\frac{l(l+1)\Phi_{lm}}{s^2} = \frac{\beta}{1+\beta}\left(\delta_{lm}^g - \frac{\mathrm{d}\log S}{\mathrm{d}s}\frac{\mathrm{d}\Phi_{lm}}{\mathrm{d}s}\right),$$

where S is the selection function and $\Phi(s)$ is the velocity potential expressed in redshift space. Boundary conditions were fixed by setting the density contrast outside the observed volume to zero. An example of how the full velocity field modulates galaxy magnitudes at $z = 0.1$ is depicted in Figure 2 (left panel). The velocity reconstructions and the method's accuracy were assessed with the help of mocks generated from the Millennium Simulation [15, 16]. Excluding the dipole in the velocity reconstruction ($l > 1$), the found distribution of β-estimates peaks at the true value $\beta_{\text{true}} = 0.52$, deviating from a symmetric Gaussian mainly because of the velocity field's nonlinear dependence on β (see right panel of Figure 2). A preliminary analysis of the SDSS data with fixed Hubble constant and density parameters from [17] yields $\beta = 0.42 \pm 0.14$ which, using the power
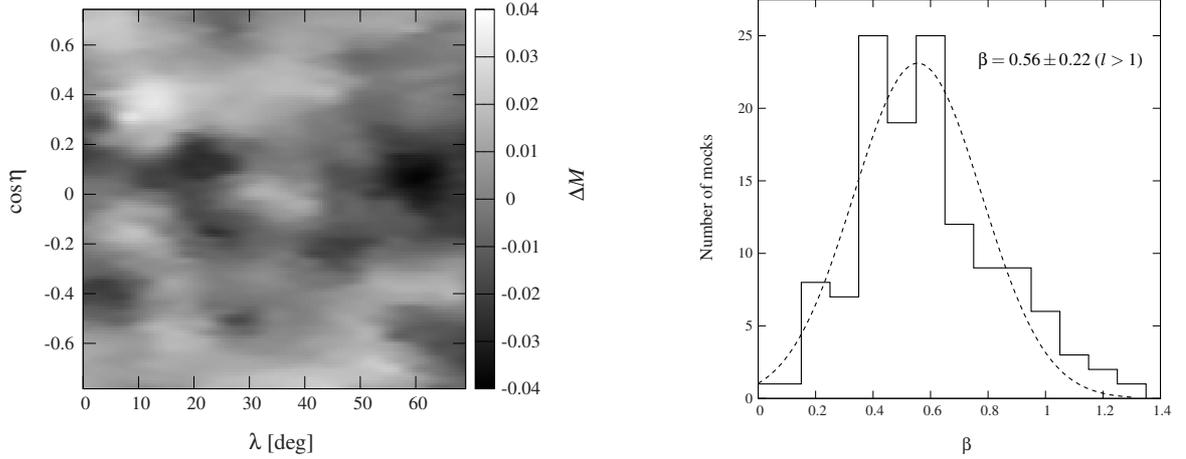
Figure 2: *Left panel.*—Velocity-induced modulation of galaxy magnitudes at $z = 0.1$ over an angular patch expressed in SDSS survey coordinates (based on a random mock). *Right panel.*—Distribution of β-estimates (and Gaussian fit) derived from mock catalogs, excluding the dipole in the velocity reconstruction ($l > 1$).

spectrum amplitude of $L^\star$-galaxies from [18], translates into $f\sigma_8 = 0.37 \pm 0.13$ and is consistent with the ΛCDM model. For samples with similar characteristics, the accuracy is comparable to what is obtained from recent measurements of anisotropic clustering in redshift space [19].

4. Outlook

Current and next-generation spectroscopic galaxy surveys are designed to reduce data-inherent systematics because of larger sky coverage and improved photometric calibration in ground- and space-based experiments [20, 21]. Together with the above results, these observational perspectives give confidence that the luminosity-based approach will be established as a standard cosmological probe, independent from and complementary to the more traditional ones based on galaxy clustering, gravitational lensing and redshift-space distortions. The method considered here does not require accurate redshifts and can also be used with photometric redshift surveys such as the 2MASS Photometric Redshift catalog (2MPZ) [22] to recover signals on scales larger than the spread of the redshift error.

References

[1] N. Kaiser, *MNRAS*, **227**, 1 (1987).

[2] A.J.S. Hamilton, *Linear Redshift Distortions: a Review*, in *The Evolving Universe, Astrophysics and Space Science Library*, **231** (1998) [`astro-ph/9708102`].

[3] D.G. York, J. Adelman, J.E. Anderson, Jr., *et al.*, *AJ*, **120**, 1579 (2000) [`astro-ph/0006396`].

[4] G.A. Tammann, A. Yahil, & A. Sandage, *ApJ*, **234**, 775 (1979).

[5] A. Nusser, E. Branchini, & M. Davis, *ApJ*, **735**, 77 (2011) [`arXiv:1102.4189`].

[6] A. Nusser, E. Branchini, & M. Davis, *ApJ*, **744**, 193 (2012) [`arXiv:1106.6145`].

[7] R.K. Sachs, & A.M. Wolfe, *ApJ*, **147**, 73 (1967).

[8] M.R. Blanton, & S. Roweis, *AJ*, **133**, 734 (2007) [`astro-ph/0606170`].

[9] K.N. Abazajian, J.K. Adelman-McCarthy, M.A. Agüeros, M.A., *et al.*, *ApJS*, **182** 543 (2009) [`arXiv:0812.0649`].

[10] M. Feix, A. Nusser, & E. Branchini, *JCAP*, **09**, 019 (2014) [`arXiv:1405.6710`].

[11] M. Feix, A. Nusser, & E. Branchini, in preparation.

[12] M.R. Blanton, D.J. Schlegel, M.A. Strauss, *et al.*, *AJ*, **129**, 2562 (2005) [`astro-ph/0410166`].

[13] N. Padmanabhan, D.J. Schlegel, D.P. Finkbeiner, *et al.*, *ApJ*, **674**, 1217 (2008) [`astro-ph/0703454`].

[14] A. Nusser, & M. Davis, *ApJ* (Letters), **421**, L1 (1994) [`astro-ph/9309009`].

[15] V. Springel, S.D.M. White, A. Jenkins, *et al.*, *Nature*, **435**, 7042 (2005) [`astro-ph/0504097`].

[16] B.M.B. Henriques, S.D.M. White, G. Lemson, *et al.*, *MNRAS*, **421**, 4 (2012) [`arXiv:1109.3457`].

[17] E. Calabrese, R.A. Hlozek, N. Battaglia, *et al.*, *Phys. Rev. D*, **87**, 10 (2013) [`arXiv:1302.1841`].

[18] M. Tegmark, M.R. Blanton, M.A. Strauss, *et al.*, *ApJ*, **606**, 2 (2004) [`astro-ph/0310725`].

[19] C. Howlett, A. Ross, L. Samushia, *et al.*, *arXiv:1409.3238* (2014).

[20] M. Levi, C. Bebek, T. Beers, *et al.*, *arXiv:1308.0847* (2013).

[21] R. Laureijs, J. Amiaux, S. Arduini, *et al.*, *arXiv:1110.3193* (2011).

[22] M. Bilicki, T.H. Jarrett, J.A. Peacock, *et al.*, *ApJS*, **210**, 9 (2014) [`arXiv:1311.5246`].